Shahid Chamran University of Ahvaz

Irrigation Sciences and Engineering (JISE)
Vol. 47, No. 4, Winter 2025, p. 105-122

Journal homepage: https://jise.scu.ac.ir

Original Paper

Comparison of sensitivity of interpolation methods by rain gauge network density

Amin Kanooni[1*] and Erfan Faraji Amogein[2]

1- Corresponding Author, Associate Professor, Department of Water Engineering, University of Mohaghegh Ardabili, Ardabil, Iran (amin.kanooni@uma.ac.ir)*
2- M. Engineering., Department of Water Engineering, University of Mohaghegh Ardabili, Ardabil, Iran.

ARTICLE INFO

Article history:
Received: 30 October 2024
Revised: 22 January 2025
Accepted: 23 January 2025

Keywords:
Density, Interpolation Methods, Inverse Distance Weight, Kriging, Rain-gauge Stations, Spatial analysis.

TO CITE THIS ARTICLE:

Kanooni, A., Faraji Amogein, E. (2025). 'Comparison of sensitivity of interpolation methods by rain gauge network density', Irrigation Sciences and Engineering, 47(4), pp. 105-122. doi: 10.22055/jise.2025.48259.2140.

Abstract

Different interpolation methods, each with their own strengths and weaknesses, are used to temporal and spatial estimation of precipitation. The accuracy of this estimate depends on the density of point data measured at rain gauge stations. In this study, the effects of the rain gauge network density on the accuracy of different interpolation methods were investigated in producing a monthly precipitation zoning map for the Samian catchment in Ardabil, Iran. The effectiveness of Bayesian Kriging, Completely Regularized Spline, Local Polynomial, Inverse Distance Weight, Ordinary Kriging, Ordinary Co-Kriging, Simple Kriging, Simple Co-Kriging, Spline with Tension, Thin Plate Spline and Universal Kriging interpolation methods was evaluated in two gauges density scenarios using evaluation criteria over 2011-2013. It was found that Inverse distance weight and Bayesian kriging methods had the best performance for the first scenario with high gauge density (16 Stations) and the second scenario with low gauge density (11 Stations), respectively. Moreover, analysis of variations in indicators across scenarios revealed that reducing the rain gauge network density by 30% improved evaluation metrics in only 40% of cases. Bayesian Kriging and Completely Regularized Splines were introduced as the preferred methods for improving evaluation indices change, and Local polynomial and simple co-Kriging methods were selected as the superior methods for improving evaluation indices quantity.

Introduction

Climate data play a significant role in modeling of water resource systems. Despite their importance, these data are not continuously available, and their statistical period may be incomplete or inconsistent with the intended study period. On the other hand, data measured at one gauging station may not cover the entire study area (Hoogenboom, 2000). Therefore, it is necessary to use interpolation methods to estimate the spatial distribution of climate variables including rainfall (Legates and McCabe Jr, 1999).

Spatial interpolation techniques are divided into two models: geostatistical and deterministic. In deterministic models, the interpolated surface is created based on the degree of similarity of the measured points and is more affected by nearby points than distant points. While geostatistical models uses statistical properties (i.e. Autocorrelation) of the measured points and assumes that the data follows a stationary stochastic process (Hadi and Tombul, 2018, Yang et al., 2015). In the past years, various interpolation methods have been employed to interpolate rainfall data and determine the best approach. Numerous studies have shown that the appropriate interpolation methods may vary from region to region (Adhikary and Dash, 2017, da Silva et al., 2019, Kumari et al., 2017, Ly et al., 2011, Plouffe et al., 2015, Xu et al., 2015). The comparison between deterministic and geostatistical techniques is performed among the studies. The results showed that the geostatistical techniques provide better rainfall estimation than deterministic techniques (Agnew and Palutikof, 2000, Vicente-Serrano et al., 2003, Buytaert et al., 2006). However, the results depend on the sampling density (Dirks et al., 1998). Four interpolation methods (Thiessen polygon, Inverse distance weight, Thin plate, and Kriging) were evaluated in Southwest England at three gauge densities through the leave-one-out cross-validation (LOOCV) method (Otieno et al., 2014). The results showed that the rain gauge density has an effect on the accuracy of the interpolated results. It was also found that the Inverse Distance Weight and Kriging interpolation methods were better than the Thiessen polygon and Thin plate methods at all the three gauge densities. Several studies have examined the effect of rain gauge density on the quality of zoning maps, including the study by Gyasi-Agyei (2020) to determine the optimal spacing between radar rain gauges. Maier et al. (2020) evaluated the effect of rain gauge density on rainfall-runoff estimation in an urban area and showed that reducing rain gauges by 50% in the rainfall-runoff model increased the error in runoff estimation by 25%. Similarly, Hohmann et al. (2021) studied the effect of rain gauge density on rainfall-runoff modeling. They evaluated six heavy rainfall events using two interpolation methods (inverse weighting of distances and tuning), and ultimately the distance between 2.5 and 4 km was considered appropriate for rain gauge stations.

Jalili Pirani and Modarres (2020) used deterministic and geostatistical algorithms (Thiessen Polygon, Inverse Distance Weighting, Ordinary Kriging, and Universal Kriging) to interpolate precipitation in the Zayandeh Roud Dam Basin (Isfahan, Iran). The results showed that Ordinary Kriging and Universal Kriging algorithms performed better in generating data when grid sizes of 27, 15 or 10 were used, while Thiessen Polygon performed better at network size of five gauges.

Gilewski (2021) studied two final interpolation methods (inverse weighting and first-order polynomials) and their effects on rainfall-runoff model results, as well as the effects of meshing and its clarity on rainfall interpolation in mountainous regions. The use of the first-order polynomial method with a grid size of 750 m proved to be the most appropriate interpolation method. Moreover, with the Inverse Distance Weight method, the selection of the inverse distance power has a stronger effect than the selection of the grid size(Gilewski, 2021).

Caloiero et al. (2021) used spatial interpolation techniques including Inverse Distance Weighting, Ordinary Kriging, External Drift Kriging, and Ordinary Cokriging to compare different spatial interpolation algorithms, both geostatistical and deterministic, in generating monthly rainfall maps in New Zealand. The results of cross-validation showed that the kriging method was better than Inverse Distance Weighting in spatial interpolation of rainfall data with geostatistical methods. According to the results, Ordinary Cokriging was identified as the best method for interpolating rainfall distribution in New Zealand for almost all months.

As an arid and semi-arid country, Iran faces several challenges in water management (Saatsaz, 2020). Khalili et al. (2016) used the Precipitation Concentration Index (PCI), to examine precipitation in the geographical area of Iran and found that precipitation is mostly classified as irregular or very irregular, particularly in winter (Khalili et al., 2016). The study of temporal and spatial changes of precipitation in Iran also indicates considerable variability of monthly precipitation. These changes occur randomly within the country, suggesting trend patterns in the north and west and random and scattered patterns in the south and east (Javari, 2017). There are three regions in Iran in terms of probability of heavy and excess rainfall, including the Caspian Sea region (north), the northwestern and western regions, and the central, eastern, and northeastern regions (Rousta et al., 2017). An analysis of rainfall in Iran conducted by Salehi et al. (2020) revealed that precipitation declined sharply between

1997 and 2016. According to recent studies, precipitation has also been declining. Ghorbani et al. (2021) investigated the spatial variation of precipitation and temperature in Ardabil province and found that most precipitation occurs in the western regions of the province and that temperature varies more than precipitation(Ghorbani et al., 2021). Reviewing the history of studies shows that each of the interpolation methods has advantages and disadvantages, and the selection of a suitable method depends on the type of data, the desired degree of accuracy, the method of performing calculations, and the climate of the study area. So, it can be said that interpolation methods are not preferred over others, but the best method should be determined for each specific area (Lam, 1983).

Since climate data play a critical role in water resource planning. Moreover, these data are not consistently available, or they may have disappeared. These factors lead to the use of various interpolation methods to produce zonal maps for climate parameters. On the other hand, due to the change in the number of stations in the study area (establishment of the rain gauge stations grid), this study specifically investigates the effect of different rain gauge density on the performance of interpolation methods and introducing preferred interpolation methods.

Materials and Methods

Study area

The study focuses on the basin overlooking the Samian hydrometric station in Ardabil province (Iran), which is part of the Qarasoo catchment (37° 55′–39° 0′ E longitude and 47° 50′–48° 55′ N latitude). The minimum and maximum altitudes above sea level are 1290 and 4790 m, respectively; and the total area is approximately 40000 km^2. The data used in this study were collected from 25 rain gaging stations between 2011 and 2013. The rainfall data were obtained from the archives of the Regional Water Company of Ardabil. Fig. (1) illustrates the location of the study area and the precipitation gaging stations distribution.

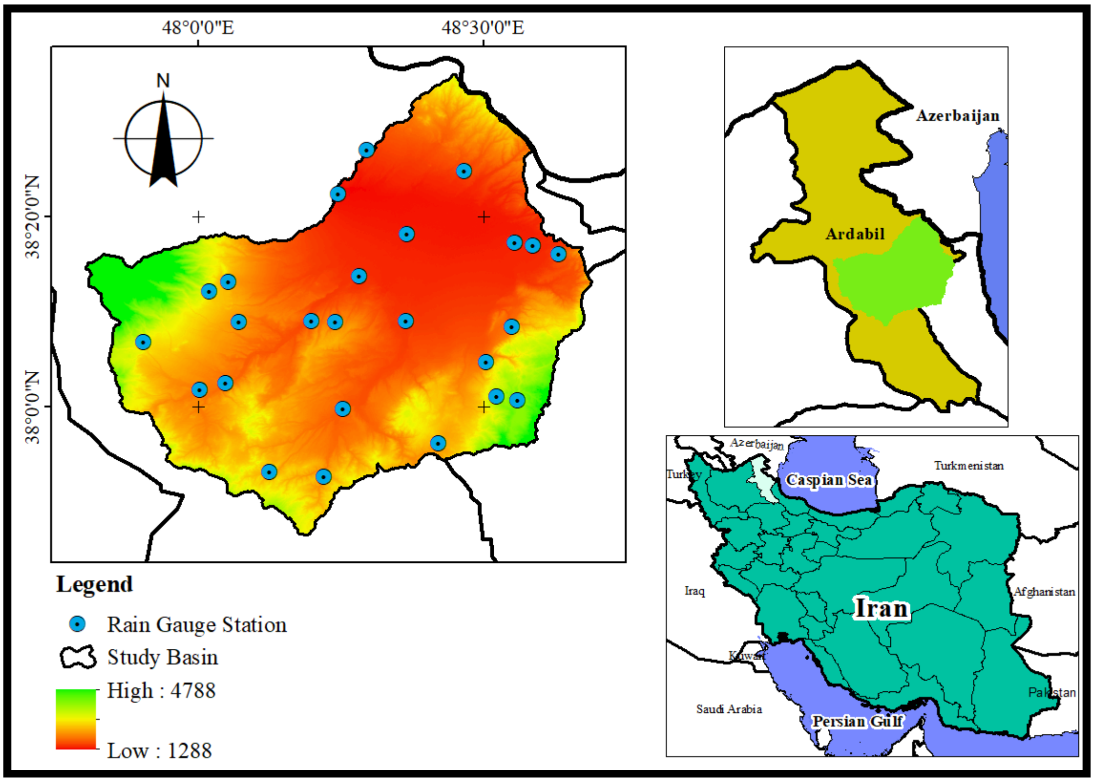

Fig. 1- Location and distribution of rain gauge stations in the study area

Methods of interpolation

As a highly variable spatiotemporal phenomenon, rainfall is often analyzed using monthly data to map precipitation zones in hydrological modeling frameworks. According to the spatial data measured at certain points, interpolation methods are used to estimate the climatic parameters in unmeasured points (Lam, 1983). In this study, different interpolation methods were used to construct the precipitation zone map and select the most suitable interpolation method. The following are the different interpolation methods used in this study:

Inverse Distance Weight (IDW)

This method is based on the assumption that the farther the distance to the point of interest, the smaller the effect on the estimate of the variable (Shepard, 1968). When *r(x,y)* is the coordinate of any point, the desired parameter estimation at the desired point in the IDW method is expressed by Eq. (1):

$$F(r) = \sum_{k=1}^{N} W(r_k) f(r_k) \quad (1)$$

Where *F(r)* is the estimated parameter value, *N* is the number of known and effective points (the number of stations), $f(r_k)$ is the actual value recorded in the points, $r_k \equiv (x_k, y_k)$ is the coordinate of the effective point, and $W(r_k)$ is the weight of the desired station obtained from Eq. (2):

$$W(r_k) = \frac{d_k(r)^{-p}}{\sum_{k=1}^{N} d_k(r)^{-p}} \quad (2)$$

Where $d_k(r)$ is the Euclidean distance between two points and *p* is the weighting power of the distance which varies between 0.25 to 100. This means that the higher the value, the greater the effect of distance. By contrast, the closer the distance, the greater the role. Eq. (3) can also be used to calculate $d_k(r)$ (Mitáš and Mitášová, 1988):

$$d_k(r) \equiv \sqrt{(x - x_k)^2 + (y - y_k)^2} \quad (3)$$

Local Polynomial (LPI)

Global polynomial interpolation fits a polynomial for the entire surface. But in local polynomial interpolation, several definite polynomials are fitted within each overlapped neighborhood. When the surface has a different shape, a single global polynomial cannot fit the surface well. Multiple polynomials have the ability to provide such surfaces with higher accuracy. In the local polynomial method, a specified order of polynomial (e.g., zeroth, first, second, and third order) fits a surface for the above neighborhood using only all points within the defined neighborhood. The neighborhoods overlap and the value used for each prediction is the value of the fitted polynomial at the center of the neighborhood. Two factors are considered key to enhancing the performance of the LPI method, including equal spacing between samples and uniform distribution of samples. The LPI method includes exponential, Gaussian, discontinuous, fixed, fourth-order polynomial, and fifth-order polynomial functions (Gribov and Krivoruchko, 2011).

Radial Basis Functions (RBF)

Radial basis function interpolation is a method to interpolate functions or data using the weighted sum of radial basis functions. The Gaussian function is one of the most widely used radial basis functions, which has been shown to approximate a wide range of functions. This method estimates a function to fit a surface of all measured points based on the change in the estimated values as a function of the distance of the measured points (Schaback, 2005).

Kriging Methods

Kriging is one of the geostatistical methods that use the spatial variance of the measured point values to estimate variable values. It is assumed that the data are spatially correlated and conform to a normal distribution (Swan, 1998). There are several types of kriging, which are described below.

Ordinary Kriging (OK)

In this method, the effects of the known points for estimation are determined to have an unbiased linear composition. Also, linear estimators have minimum variance. This estimator is defined as Eq. (4):

$$\hat{Z}_{OK}(u) = \sum_{i=1}^{n(u)} \lambda_i^{OK} . Z(u_i) \quad (4)$$

Where $\hat{Z}(u)$ is the estimated value at u, λ_i is the weight assigned to the variable at point u_i, $Z(u_i)$ is the value of the spatial variable in sample i, and $n(u)$ is the number of observation points (Hutchinson, 1993).

Simple Kriging (SK)

Besides the assumptions of the Ordinary Kriging method, this method of estimating the value of a variable has other assumptions, including independence of coordinates, no trend in the data, and knowing the mean value of the variable ($m(u)$). Eq. (5) can be used to estimate the value of a parameter at a given point.

$$\hat{Z}_{SK}(u) = m(u) + \sum_{i=1}^{n(u)} \lambda_i(u)[Z(u_i) - m(u_i)] \quad (5)$$

Where $\hat{Z}(u)$ is the value estimated at u, λ_i is the weight attributed to the variable at point u_i, $Z(u_i)$ is the value of the spatial variable in sample i, and $n(u)$ is the number of observation points (Swan, 1998).

Co-Kriging (CoK)

A correlated variable can serve as a backup variable in kriging methods when there is a correlation between the desired variable and another variable. This feature can also be used when there is not enough data for a variable to provide more accurate results. Eq. (6) is defined as the equation for estimating the value of the relevant variable

$$\hat{Z}_{COK}(u) = \sum_{i=1}^{n(u)} \lambda_i(u) Z(u_i) + \sum_{j=1}^{m(u)} w_j^{COK}(u) e(u_j) \quad (6)$$

Where $\hat{Z}(u)$ is the value estimated at u, λ_i is the weight assigned to the principal variable at point u_i, $Z(u_i)$ is the value of the principal variable in sample i, w_j^{COK} is the weight of the auxiliary variable, $e(u_j)$ the observed value of the auxiliary variable, $m(u)$ is the number of even points of the auxiliary variable and $n(u)$ is the number of observation points (Isaaks and Srivastava, 1989).

Universal Kriging (UK)

Universal Kriging can be seen as a point interpolation, which requires a point map as input and which returns a raster map with estimations and optionally an error map. Matheron (1969) introduced universal kriging as a special case of kriging that models the process as a function of coordinates. Universal Kriging is Kriging with a local trend. The local trend or drift is a continuous and slowly varying trend surface on top of which the variation to be interpolated is superimposed. The trends in the data are first identified and deleted, then estimates are made based on the remaining data that do not trends, and finally the deleted values are added to the estimated values (Zimmerman et al., 1999).

Bayesian Kriging (BK)

Bayesian Kriging is the most different method of Kriging. It uses a rotation method and the parameter is estimated several times. Since it does not respond to moving averages, it has a wider range of changes and can also detect sudden variations (Mirzaei and Sakizadeh, 2016).

The comparison between Bayesian and Ordinary Kriging methods

Bayesian Kriging and Ordinary Kriging are both geostatistical methods used for spatial interpolation, but they differ primarily in how they handle uncertainty and incorporate prior knowledge. Bayesian Kriging incorporates prior distributions and models the uncertainty associated with the estimates, allowing for the integration of prior knowledge about the spatial process. Ordinary Kriging, on the other hand, does not use prior distributions and relies solely on observed data to make predictions. Bayesian Kriging explicitly quantifies uncertainty in the predictions through posterior distributions, which provides a more comprehensive understanding of variability. Ordinary Kriging provides point estimates and assumes that the uncertainty can be addressed through the variogram, often giving less insight into the overall confidence of predictions. Bayesian Kriging can be particularly effective in scenarios with small datasets, where incorporating prior information could enhance the accuracy of predictions. Ordinary Kriging typically performs well with larger datasets where spatial autocorrelation is well-defined.

Validation of the interpolation methods

To evaluate the accuracy of the different interpolation methods, the mean bias error (*MBE*), mean absolute error (*MAE*), mean squared error (*MSE*), Willmott's *D*-index, model efficiency (*ME*), and correlation coefficient (R^2) of the interpolated values were calculated with the following equations:

$$MBE = \frac{1}{N_A}\sum_{k=1}^{N_A}[F(r_k) - f(r_k)] \quad (7)$$

$$MAE = \frac{1}{N_A}\sum_{k=1}^{N_A}|F(r_k) - f(r_k)| \quad (8)$$

$$MSE = \frac{1}{N_A}\sum_{k=1}^{N_A}[F(r_k) - f(r_k)]^2 \quad (9)$$

$$ME = 1 - \frac{\sum_{k=1}^{N_A}[F(r_k)-f(r_k)]^2}{\sum_{k=1}^{N_A}\left[f(r_k)-\overline{f(r)}\right]^2} \quad (10)$$

$$D = 1 - \frac{\sum_{k=1}^{N_A}\left[F(r_k)-\overline{f(r)}\right]^2}{\sum_{k=1}^{N_A}\left[F(r_k)-\overline{f(r)}\right]\sum_{k=1}^{N_A}\left[f(r_k)-\overline{f(r)}\right]} \quad (11)$$

$$R^2 = \left\{1 - \frac{\sum_{k=1}^{N_A}\left[F(r_k)-\overline{f(r)}\right]\left[f(r_k)-\overline{f(r)}\right]}{\sqrt{\sum_{k=1}^{N_A}\left[F(r_k)-\overline{f(r)}\right]^2}\sqrt{\sum_{k=1}^{N_A}\left[f(r_k)-\overline{f(r)}\right]^2}}\right\}^2 \quad (12)$$

Where $f(r_k)$ is the value observed at the test points, $r_k \equiv (x_k, y_k)$ is the coordinate of the points, $F(r_k)$ is the estimated value of the test point, $\overline{f(r)}$ is the mean of the observed values and N_A is the number of test points.

All indices have different meanings and complement each other to allow an accurate evaluation of the different interpolation methods. If *MBE*, *MAE* and *MSE* are closer to zero, the better the model. To calculate the error in the *MBE* index, it is necessary to sample at the population level, not for a single station. It is used as a supplement to the *MSE* index, which is sensitive to large errors. *MAE* index can also be calculated using both estimated and observed averages and is one of the most reliable evaluation methods (Hernandez-Stefanoni and Ponce-Hernandez, 2006, Krause et al., 2005). The *ME* index is used to express possible biases. Since it considers both positive and negative values together, the value of this index is constantly lower than the actual error(Li and Heap, 2008).

Selection which measures to use for regression problems depends on the data, the model, and the objective. When the conditional distribution of observations is asymmetric, for an unbiased fit, the *MSE* is minimized by the conditional mean, and the *MAE* is minimized by the conditional median. To put it in short, *MAE* is robust to outliers, meaning that it is not affected by extreme errors. It has the same unit as the target variable, making it easy to compare . However, it does not penalize large errors as much as small errors, meaning that it might not reflect the true accuracy of the model. In general, *MAE* is a simple and intuitive metric that is robust to outliers, but *MSE* is a measure that reflects the true accuracy of the model and is easy to optimize.

The validation and evaluation processes are performed using Willmott's *D*-index. This index does not consider outliers based on criteria (observed values) (Willmott, 1982). To express the correlation between the observed values and the predicted values, the coefficient of determination (R^2) is usually used, which is a common performance measure. However, it is not recommended to be used as a measure of model performance because it is insufficient and often misleading. If *ME*, *D* and R^2 are closer 1, the method is considered more accurate (Vicente-Serrano et al., 2003).

The best interpolation method selection process

The current rain gauging stations were divided into two categories of control and observation ones to evaluate the ability of different interpolation methods in rainfall zoning. Control stations were selected to ensure a spread of stations across the region. They accounted for about 30% (8 stations) of the total stations. Then, the observation stations were divided into two scenarios based on the length of the available statistical period. To investigate how the reduction in the number of rainfall gauging stations affects the appropriate interpolation selection, 16 and 11 stations were considered in the first and second scenarios, respectively. The stations with a longer statistical period were grouped in the second scenario. Selection of gauges was carefully done to ensure that the catchment was still reasonably covered by the rain gauge stations. The resulting spatial distributions of the gauges at the two densities scenarios are shown in Fig. (2). The details of the stations also were listed in Table (1).

Using a variety of interpolation methods (11 methods), monthly zonal maps (for 36 months) were derived for each scenario (792 maps) and precipitation values were estimated at control stations. For each scenario, we calculated the evaluation indicators of the interpolation methods for different months. The interpolation method was selected based on the difference between the values of the corresponding monthly indicators in the two scenarios, as shown in Fig. (3).

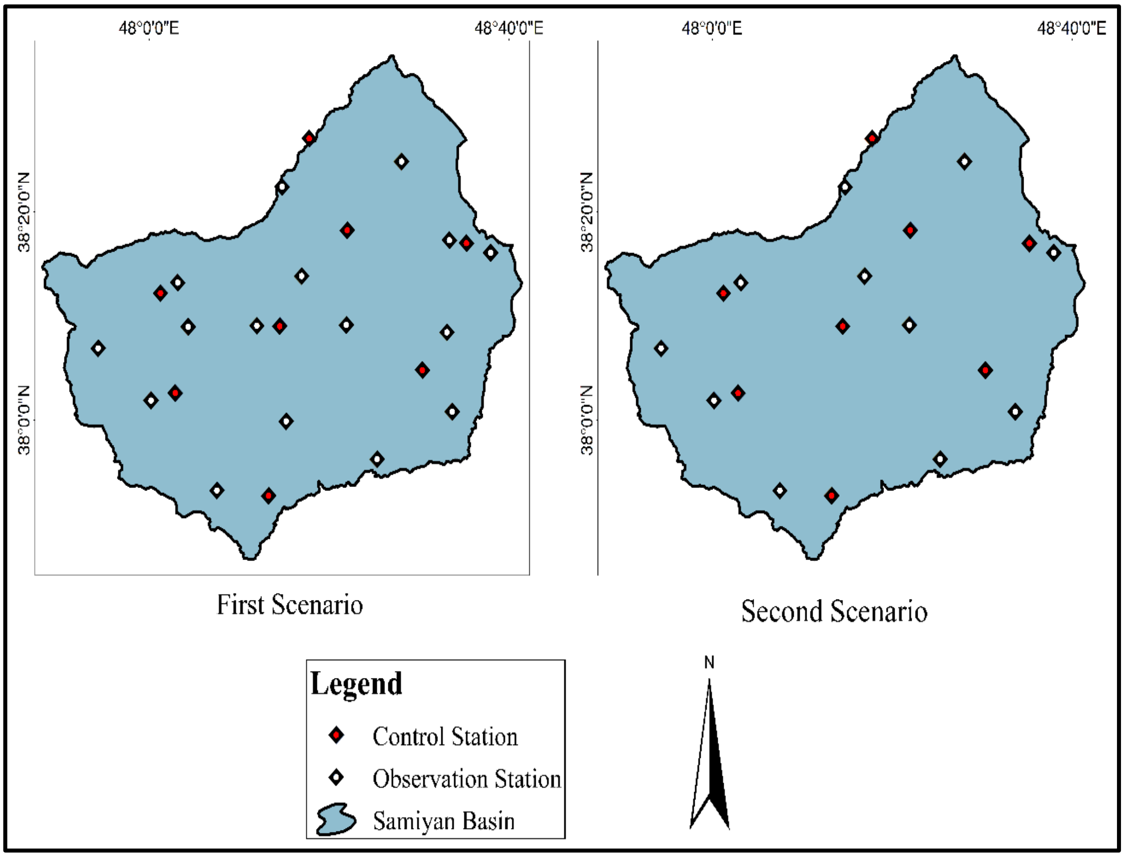

Fig. 2- The spatial spread of the stations in two densities scenarios in the study area.

Table 1. Details of stations located in the study area

Station	Geographical location		Established	Stations for scenarios		
	X	Y	year	Control	Scenario I	Scenario II
Sarein	243500	4223500	1992	×	✓	×
Niaraq	291958	4238139	1972	×	✓	✓
Hir	281366	4217779	1997	✓	×	×
Atashgah	242462	4233885	1973	×	✓	✓
Baghrabad	285791	4242187	2001	×	✓	×
Saein	282482	4227591	2000	✓	×	×
Hellabad	273494	4202106	1972	×	✓	✓
Tutunsiz	247288	4197072	1970	×	✓	✓
Goli	253386	4190838	2009	✓	×	×
Abibagloo	286259	4240601	1999	×	✓	×
Ardabil	262138	4234888	1971	×	✓	✓
Polealmas	254599	4226257	2000	×	✓	×
Samian	259426	4250859	1972	×	✓	✓
Siahpoosh	255619	4195955	1995	✓	×	×
Shamsabad	258868	4209127	2000	×	✓	×
Kuzetopraqi	269137	4225954	1972	×	✓	✓
Gilandeh	269763	4242813	1998	✓	×	×
Lay	228700	4223071	1979	×	✓	✓
MollaAhmad	264071	4259331	1999	✓	×	×
Namin	278893	4254806	1971	×	✓	✓
Nir	237000	4213500	1973	×	✓	✓
Neor	285943	4210069	1973	×	✓	✓
Yamchi Olia	240950	4214706	1998	✓	×	×
Aladizga	289090	4240064	1997	✓	×	×

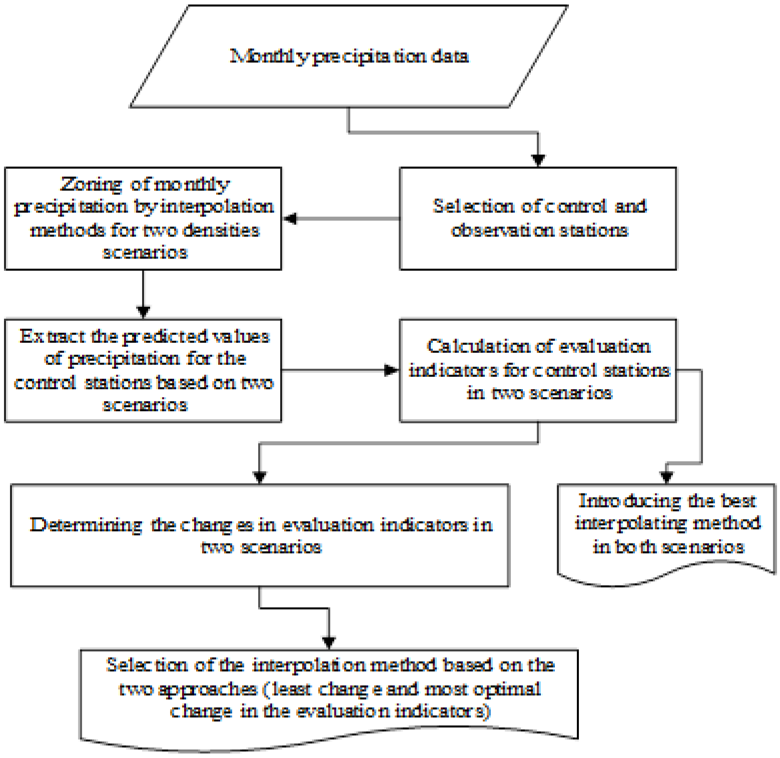

Fig. 3- The process of selecting the preferred interpolation method at two densities scenarios

In examining the change in evaluation indicators in the two scenarios, two approaches were considered based on the characteristics of each evaluation indicator (Fig. 3). In the first approach, the change of the evaluation indicators (according to their sign) was investigated, indicating that changes in the two scenarios could either improve or weaken the interpolation results. Secondly, the quantitative values of the index changes were examined, and the method with the smallest change was determined to be superior. In this context, Eqs. (13), (14), and (15) were used. Eq. (13) was used to evaluate how to change the error calculation indices (Eqs. 7, 8, and 9), while Eq. 14 was used to evaluate how to change the performance calculation indices (Eqs. 10, 11 and 12).

$$Z_m^n = |A_m^n| - |B_m^n| \tag{13}$$

$$Z_m^n = |A_m^n - 1| - |B_m^n - 1| \tag{14}$$

Where A and B are the calculated values of the corresponding evaluation index in the first and second scenarios, respectively; *n* represents the number of the month, which can be a value in the interval of (Hoogenboom, 2000, Willmott, 1982), *m* represents the interpolation method, and *Z* represents the difference of the desired index associated with the interpolation method *m* in month *n*. When *Z* is less than zero, the interpolation method is weaker, with changing the first scenario to the second one (fewer stations). Whereas, if *Z* has a value of zero, changing the scenario does not affect the evaluation indicators. Furthermore, when *Z* has a value greater than zero, reducing the number of stations helps improve the evaluation indicators.

Eq. (15) was also used to determine the quantitative change in evaluation indicators between the two scenarios.

$$Q_m^n = \big||A_m^n| - |B_m^n|\big| \tag{15}$$

Where *Q* represents the difference between the corresponding evaluation index in the first and second scenarios. *Q* is always greater than or equal to zero. By reducing the number of stations, an appropriate interpolation method can be selected that yields the least change in results using Equation 15. The process of selecting an appropriate interpolation method for low density gauging stations (the second scenario compared to the first one) has been illustrated in Fig. (4).

Results and Discussion

Using the monthly precipitation values during the statistical period in the first scenario, the evaluation indicators were calculated for all months. As shown in Table (2), which summarizes the evaluation indicators, it can be concluded that the IDW method with lower values of model accuracy measurement indices (*MAE*=10.76, *MBE*=-7.0 & *MSE*=289.33) was generally an appropriate method. Following this method, the local polynomial with Gaussian trend performed well in the monthly evaluations. The *MBE* index is always less than zero for all methods, which can be seen from Eq. 7 that the interpolation methods provide a lower estimate of the actual values (Table 2). Investigating the efficiency of interpolation methods based on the coefficient of determination (R^2) and the *ME* indices showed that the IDW method is the best method in interpolating the monthly precipitation values, but there is no agreement regarding the Willmott's *D*-index (R^2=*0.61*, *ME*=0.44). An example of a zone map extracted in April 2011 using the two preferred methods (IDW and local polynomial) is shown in Fig. (5).

The *MSE* and *MAE* provide a measure of interpolation precision, with lower values indicating more precise methods, while the *ME* measures the bias. The *ME* shows that bias is very small (near zero) for Completely Regularized Spline (0.12) method, whereas IDW method (0.44) have considerably more bias.

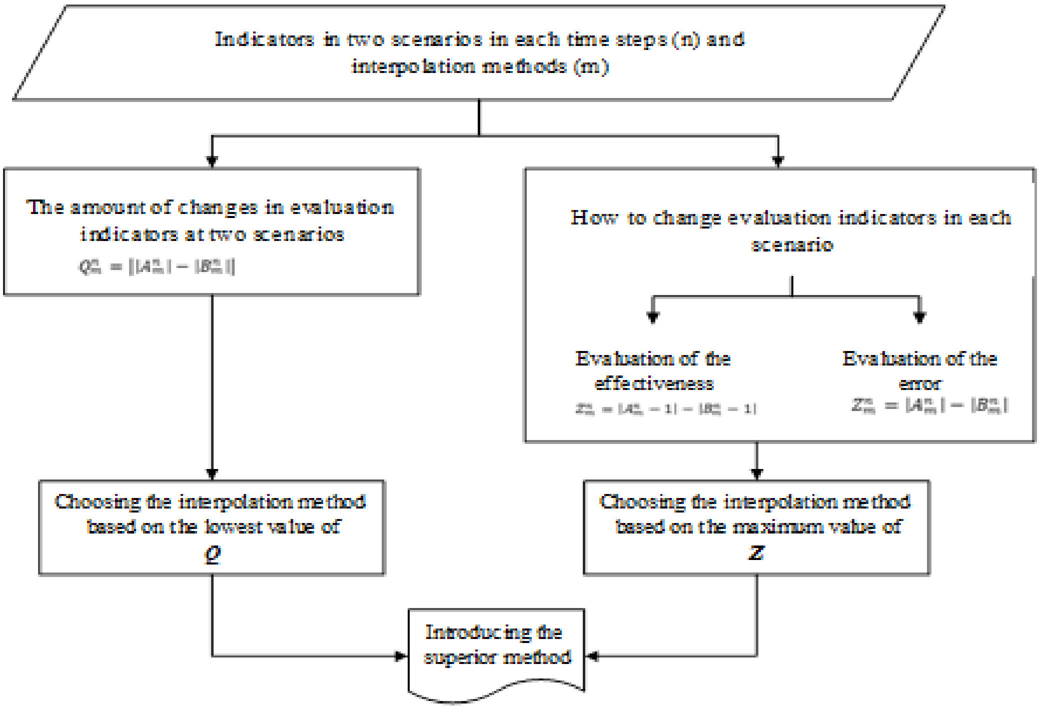

Fig. 4- Examining the change of evaluation indices to select the superior interpolation method

Table 2- The average values of evaluation indicators in the first scenario

Interpolation method	Evaluation criteria					
	D	*ME*	*MAE* (mm)	*MBE* (mm)	*MSE* (mm)	R^2
Bayesian Kriging	0.67	0.40	12.47	-6.51	341.97	0.59
Completely Regularized Spline	0.67	0.12	14.70	-10.42	495.38	0.53
Local Polynomial	0.72	0.39	11.61	-7.64	319.18	0.59
IDW	0.74	0.44	10.76	-7.00	289.33	0.61
Ordinary Kriging	0.67	0.34	12.46	-7.94	387.76	0.59
Ordinary Co-Kriging	0.65	0.34	12.70	-9.18	386.38	0.57
Simple Kriging	0.62	0.39	12.33	-8.68	356.02	0.57
Simple Co-Kriging	0.60	0.35	13.00	-8.89	378.61	0.54
Spline with Tension	0.75	0.42	11.10	-7.63	305.94	0.61
Thin Plate Spline	0.76	0.37	11.95	-7.81	322.81	0.60
Universal Kriging	0.68	0.30	13.55	-7.61	487.05	0.60

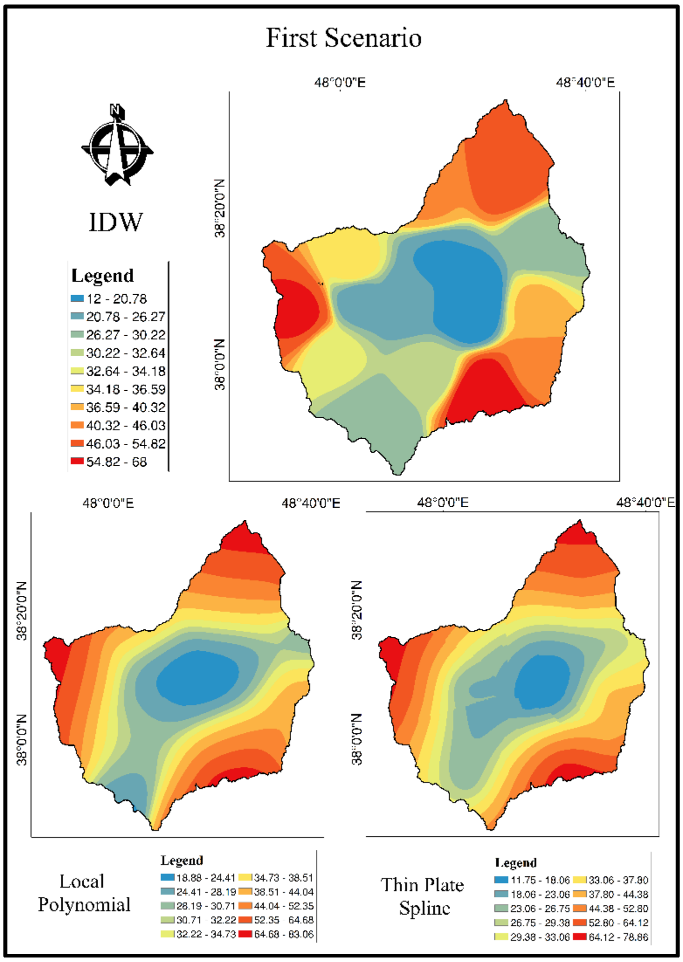

Fig. 2- Zoning of monthly precipitation (mm) by the selected method in the first scenario

As for the second scenario, with 11 rain gauges, the Bayesian Kriging method performed superior to others. Following that, the Completely Regularized Spline, Local Polynomial, Ordinary Co-Kriging, and Spline with Tension methods were ranked next. Table (3) shows the mean values of the evaluation criteria of the second scenario during the study period. When comparing the *MBE* index with its negative values, it can be seen that the estimates are often lower than the observed value. Fig. (6) also shows the maps of precipitation zones in April 2011 with selected methods.

Using equations (13) and (14) and the algorithm described in Fig. (3), we calculated the differences in evaluation indicators over the statistical period (monthly) in different station densities scenarios. The average difference between the evaluation indicators in the two scenarios (second scenario compared to the first one) is shown in Table (4). There is little difference between the evaluation indicators in the scenarios (except for the *MSE* index and one case of the *D* index). Because changing in the R^2 and *MAE* indices are often negative, the interpolation methods in the first scenario can be more effective than the other one. In other words, given that the change in the evaluation indices has been negative, the values of the indices in the first scenario have been better than the second scenario. This means that reducing the station density weakens the efficiency of the interpolation methods.

By examining the monthly difference of all indicators in the different scenarios, it can be said that in 39.8 percent of cases, better results were obtained by reducing the number of stations (second scenario), while in 0.6 percent of cases, there was no change in the evaluation results. Additionally, in 59.6 percent of cases, reducing the number of stations (second scenario) did not improve the results. Both Bayesian Kriging and Completely Regularized Spline methods yielded the most desirable changes, which can be confirmed by choosing the superior method in the first and second scenarios.

Table 3- Mean values of evaluation indicators in the second scenario

Interpolation method	Evaluation criteria					
	D	*ME*	*MAE* (mm)	*MBE* (mm)	*MSE* (mm)	R^2
Bayesian Kriging	0.78	0.31	9.45	-4.30	226.36	0.71
Completely Regularized Spline	0.74	0.35	12.08	-7.43	322.06	0.59
Local Polynomial	0.74	0.36	12.21	-8.10	323.43	0.59
IDW	0.72	0.21	13.12	-9.05	381.73	0.57
Ordinary Kriging	0.68	0.38	12.50	-8.24	357.27	0.56
Ordinary Co-Kriging	0.66	0.39	12.88	-8.55	375.24	0.56
Simple Kriging	0.59	0.30	13.89	-10.83	456.13	0.55
Simple Co-Kriging	0.59	0.30	14.04	-10.84	458.77	0.55
Spline with Tension	0.70	0.34	12.26	-8.81	337.90	0.59
Thin Plate Spline	0.75	0.29	12.82	-8.27	346.03	0.59
Universal Kriging	0.68	0.36	12.67	-8.59	366.41	0.56

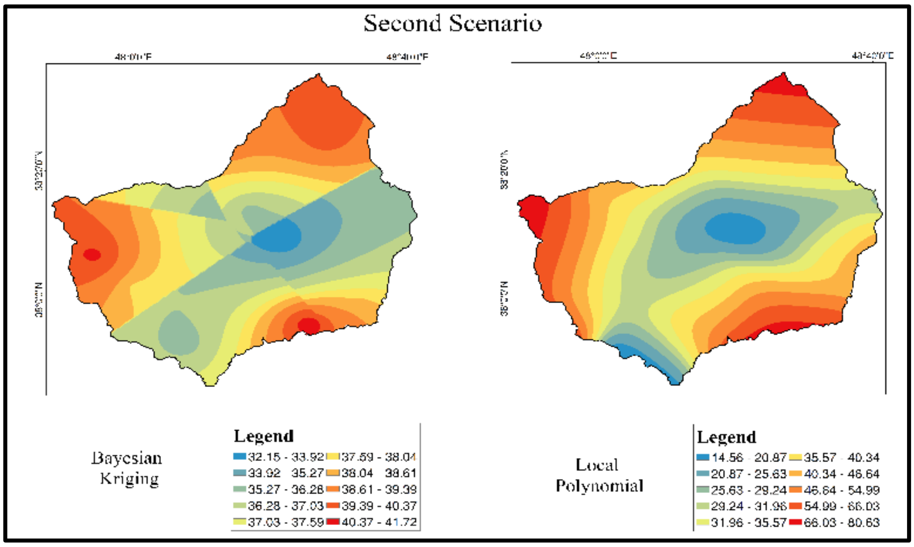

Fig. 3- Zoning of monthly precipitation (mm) by selected methods in the second scenario

The HeatMap (Fig. 7&8) shows how the evaluation indicators change monthly. In the first months of the study period, the most changes in the evaluation indices were observed, which in most cases improved the results. This means that the relevant indicators have converged to their optimal level. Then, at the end of the study period (from the middle of 2012 onwards), the changes of the indicators have decreased which indicates the deterioration of the evaluation indicators from the first scenario to the second scenario. As shown in Fig (7) and 8, the largest change in the error evaluation indices was related to the *MSE* index, indicating the most error increase between the two scenarios. As for the performance evaluation indicators, except for a few cases related to the *D*-index, the indicators have generally changed in favor of better performance.

Table 4- Monthly average of changing in evaluation indices

Interpolation method	Evaluation index					
	D	*ME*	*MAE* (mm)	*MBE* (mm)	*MSE* (mm)	R^2
Bayesian Kriging	0.11	-0.10	3.01	2.53	115.61	0.12
Completely Regularized Spline	0.07	0.22	2.64	3.87	167.19	0.06
Local Polynomial	0.02	-0.03	-0.63	-0.53	-6.50	-0.01
IDW	-0.02	-0.22	-2.37	-2.06	-92.40	-0.04
Ordinary Kriging	0.01	0.04	-0.05	0.40	30.49	-0.03
Ordinary Co-Kriging	0.01	0.05	-0.17	0.58	11.14	-0.02
Simple Kriging	-0.03	-0.09	-1.56	-2.21	-100.11	-0.02
Simple Co-Kriging	-0.01	-0.05	-1.04	-2.01	-80.16	0.01
Spline with Tension	-0.04	-0.08	-1.17	-1.07	-31.97	-0.02
Thin Plate Spline	-0.01	-0.08	-0.87	-0.47	-23.22	-0.01
Universal Kriging	0.00	0.06	0.88	1.11	120.64	-0.03

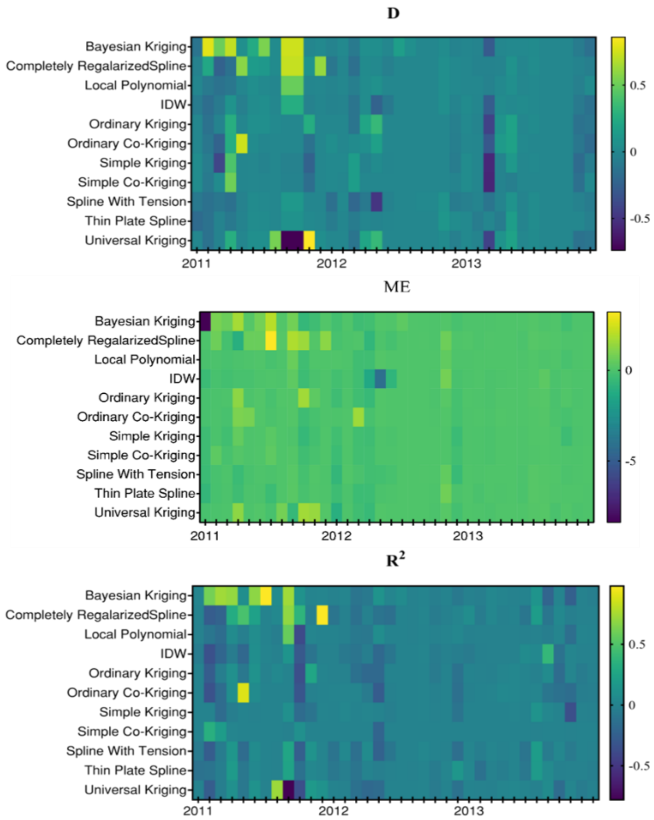

Fig. 4-. Temporal changes of how efficiency evaluation indicators change in the second scenario compared to the first (z change)

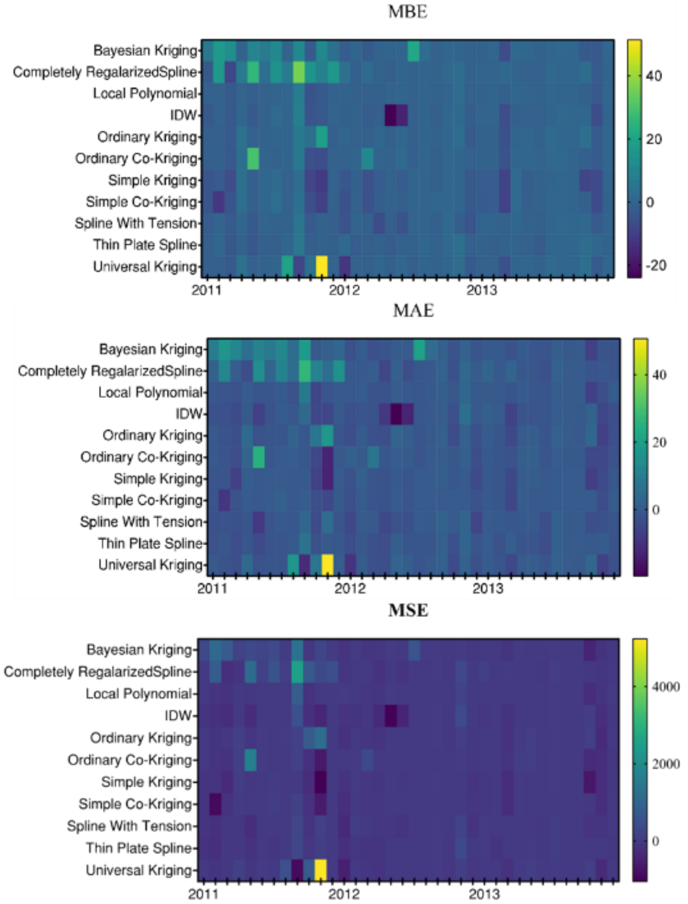

Fig. 8- Temporal changes of how error evaluation indicators change in the second scenario compared to the first (z change)

Table 5- Monthly average of changing in quantity of evaluation indices

Interpolation method	Evaluation index					
	D	*ME*	*MAE* (mm)	*MBE* (mm)	*MSE* (mm)	R^2
Bayesian Kriging	0.15	0.11	2.54	2.83	107.09	0.06
Completely Regularized Spline	0.12	0.42	2.81	3.33	144.14	0.07
Local Polynomial	0.05	0.14	1.70	1.59	71.11	0.05
IDW	0.06	0.14	2.09	2.18	90.27	0.05
Ordinary Kriging	0.07	0.17	2.46	2.03	99.60	0.05
Ordinary Co-Kriging	0.08	0.13	2.13	1.85	83.83	0.06
Simple Kriging	0.07	0.14	2.02	1.98	105.27	0.07
Simple Co-Kriging	0.05	0.25	2.17	3.00	119.72	0.05
Spline with Tension	0.07	0.21	2.41	2.26	117.81	0.09
Thin Plate Spline	0.04	0.29	2.77	3.20	157.24	0.13
Universal Kriging	0.14	0.41	6.11	5.80	364.59	0.20

To examine the quantitative change in evaluation indicators under different scenarios, Eq. 15 and the algorithm described in Fig. (3) were also used. Table (5) displays the average monthly results of this evaluation. Accordingly, with reducing the number of rain gauge stations (the second scenario compared to the first), the smallest change in the indicators (regardless of their sign) were related to the Local Polynomial and Simple Co-Kriging methods. This can be due to the slight change in the evaluation criteria for interpolation methods (Table 5). The R^2 and *D* indicators had the lowest and highest quantity change values, respectively, among the performance evaluation indicators. Also, the highest and lowest quantity changes among the error evaluation indicators are allocated to the *MAE* and *MSE* indicators.

Conclusion

Interpolation methods have different application characteristics and the output results of those methods affect hydrological modeling. In this study, the effect of different rain gauge densities on the selection of an appropriate method for interpolation and zoning of monthly precipitation was investigated. The interpolation methods, including deterministic and geostatistical methods, were examined in two scenarios with different indicators. The results showed that in conditions with high rain gauge density, deterministic methods performed better than geostatistical methods in monthly rainfall interpolation. While in low density conditions, geostatistical methods showed better performance. IDW, a deterministic method, was found to be the best interpolation methods if there is a high density of rain gauge stations. In low density rain gauge condition, the Bayesian Kriging, a geostatistical method, is preferable for interpolation purposes compared to other methods. Two methods are preferred to improve the change of evaluation indicators, such as Bayesian Kriging and Completely Regularized Spline. In addition, Local Polynomial and Simple Co-Kriging methods were chosen to improve the quantity of evaluation indicators. They performed better compared to the scenario with a smaller number of rain gauge stations. Overall, the Local Polynomial interpolation method can be considered as a suitable interpolation method regardless of the number of rain gauge stations. While when the number of stations is low, the Bayesian Kriging method can be used as the preferred interpolation method for calculating monthly precipitation. This study has provided useful results in choosing rainfall interpolation methods with various rain gauge density. To find similar patterns in other catchment, more studies should be done with different rain gauge network density.

To design rain gauge networks for real-world applications, it is essential to consider a sufficient density of gauges to capture spatial variability. This can be determined through spatial analysis of rainfall data and modeling. After selecting the appropriate rain gauge density, the appropriate interpolation method can ensure reliable results in rainfall estimation.

Data Availability Statement

Meteorological data are used from the Regional Water Company of Ardabil (www.arrw.ir) and are available from the corresponding author upon reasonable request.

Acknowledgment

The authors acknowledge Ardabil Regional Water Company for making available the meteorological data set used in this study.

References

1- Adhikary, P.P. and Dash, C.J., 2017. Comparison of deterministic and stochastic methods to predict spatial variation of groundwater depth. *Applied Water Science*, 7, pp.339-348.

2- Agnew, M.D. and Palutikof, J.P., 2000. GIS-based construction of baseline climatologies for the Mediterranean using terrain variables. *Climate research*, *14*(2), pp.115-127.

3- Buytaert, W., Celleri, R., Willems, P., De Bievre, B. and Wyseure, G., 2006. Spatial and temporal rainfall variability in mountainous areas: A case study from the south Ecuadorian Andes. *Journal of Hydrology*, 329(3-4), pp.413-421. doi.org/10.1016/j.jhydrol.2006.02.031.

4- Caloiero, T., Pellicone, G., Modica, G. and Guagliardi, I., 2021. Comparative analysis of different spatial interpolation methods applied to monthly rainfall as support for landscape management. *Applied Sciences*, *11*(20), p.9566.. https://doi.org/10.3390/app11209566.

5- da Silva, A.S.A., Stosic, B., Menezes, R.S.C. and Singh, V.P., 2019. Comparison of interpolation methods for spatial distribution of monthly precipitation in the state of Pernambuco, Brazil. *Journal of Hydrologic Engineering*, *24*(3), p.04018068. doi.org/10.1061/(ASCE)HE.1943-5584.000174.

6- Dehghani, M., Salehi, S., Mosavi, A., Nabipour, N., Shamshirband, S. and Ghamisi, P., 2020. Spatial analysis of seasonal precipitation over Iran: Co-variation with climate indices. *ISPRS International Journal of Geo-Information*, *9*(2), p.73. doi.org/10.3390/ijgi9020073.

7- Dirks, K.N., Hay, J.E., Stow, C.D. and Harris, D., 1998. High-resolution studies of rainfall on Norfolk Island: Part II: Interpolation of rainfall data. *Journal of Hydrology*, *208*(3-4), pp.187-193. doi.org/10.1016/S0022-1694(98)00155-3.

8- Ghorbani, M.A., Mahmoud Alilou, S., Javidan, S. and Naganna, S.R., 2021. Assessment of spatio-temporal variability of rainfall and mean air temperature over Ardabil province, Iran. *SN Applied Sciences*, *3*, pp.1-10.

9- Gilewski, P., 2021. Impact of the grid resolution and deterministic interpolation of precipitation on rainfall-runoff modeling in a sparsely gauged mountainous catchment. *Water*, *13*(2), p.230. doi.org/10.3390/w13020230.

10- Gribov, A. and Krivoruchko, K., 2011. Local polynomials for data detrending and interpolation in the presence of barriers. *Stochastic environmental research and risk assessment*, *25*, pp.1057-1063.

11- Hadi, S.J. and Tombul, M., 2018. Comparison of spatial interpolation methods of precipitation and temperature using multiple integration periods. *Journal of the Indian Society of Remote Sensing*, *46*, pp.1187-1199.

12- Hernandez-Stefanoni, J.L. and Ponce-Hernandez, R., 2006. Mapping the spatial variability of plant diversity in a tropical forest: comparison of spatial interpolation methods. *Environmental monitoring and assessment*, 117, pp.307-334.

13- Hohmann, C., Kirchengast, G., Sungmin, O., Rieger, W., and Foelsche, U. 2021. Small Catchment Runoff Sensitivity to Station Density and Spatial Interpolation: Hydrological Modeling of Heavy Rainfall Using a Dense Rain Gauge Network. *Water*, 13(10), 1381. doi.org/10.3390/w13101381

14- Hoogenboom, G., 2000. Contribution of agrometeorology to the simulation of crop production and its applications. *Agricultural and forest meteorology*, *103*(1-2), pp.137-157. doi.org/10.1016/S0168-1923(00)00108-8.

15- Hutchinson, M. 1993. On thin plate splines and kriging. *Computing science and statistics*, 55-55.

16- Isaaks, E. H. & SRIVASTAVA, R. 1989. An introduction to applied geostatistics. *Oxford University Press, New York*.

17- Jalili Pirani, F. and Modarres, R., 2020. Geostatistical and deterministic methods for rainfall interpolation in the Zayandeh Rud basin, Iran. *Hydrological Sciences Journal*, *65*(16), pp.2678-2692. https://doi.org/10.1080/02626667.2020.1833014.

18- Javari, M. 2017. Spatial variability of rainfall trends in Iran. *Arabian Journal of Geosciences*, 10, 78.

19- Khalili, K., Tahoudi, M.N., Mirabbasi, R. and Ahmadi, F., 2016. Investigation of spatial and temporal variability of precipitation in Iran over the last half century. Stochastic *Environmental Research and Risk Assessment*, 30, pp.1205-1221.

20- Krause, P., Boyle, D.P. and Bäse, F., 2005. Comparison of different efficiency criteria for hydrological model assessment. *Advances in geosciences*, *5*, pp.89-97. doi.org/10.5194/adgeo-5-89-2005.

21- Kumari, M., Singh, C.K. and Basistha, A., 2017. Clustering data and incorporating topographical variables for improving spatial interpolation of rainfall in mountainous region. *Water Resources Management*, *31*, pp.425-442.

22- Lam, N.S.N., 1983. Spatial interpolation methods: a review. *The American Cartographer*, *10*(2), pp.129-150. doi.org/10.1559/152304083783914958.

23- Legates, D.R. and McCabe Jr, G.J., 1999. Evaluating the use of "goodness-of-fit" measures in hydrologic and hydroclimatic model validation. *Water resources research*, *35*(1), pp.233-241. doi.org/10.1029/1998WR900018.

24- Li, J. and Heap, A.D., 2008. A review of spatial interpolation methods for environmental scientists.

25- Ly, S., Charles, C. and Degre, A., 2011. Geostatistical interpolation of daily rainfall at catchment scale: the use of several variogram models in the Ourthe and Ambleve catchments, Belgium. *Hydrology and Earth System Sciences*, *15*(7), pp.2259-2274. doi.org/10.5194/hess-15-2259-2011.

26- Matheron, G. 1969. Le krigeage universel (Universal kriging) Vol. 1. Cahiers du Centre de Morphologie Mathematique, Ecole des Mines de Paris, Fontainebleau, 83 p. https://doi.org/10.1016/j.geoderma.2003.08.018

27- Mirzaei, R. and Sakizadeh, M., 2016. Comparison of interpolation methods for the estimation of groundwater contamination in Andimeshk-Shush Plain, Southwest of Iran. *Environmental Science and Pollution Research*, *23*, pp.2758-2769.

28- Mitáš, L. and Mitášová, H., 1988. General variational approach to the interpolation problem. *Computers & Mathematics with Applications*, 16(12), pp.983-992. doi.org/10.1016/0898-1221(88)90255-6.

29- Otieno, H., Yang, J., Liu, W. and Han, D., 2014. Influence of rain gauge density on interpolation method selection. *Journal of Hydrologic Engineering*, *19*(11), p.04014024. doi.org/10.1061/(ASCE)HE.1943-5584.0000964.

30- Plouffe, C.C., Robertson, C. and Chandrapala, L., 2015. Comparing interpolation techniques for monthly rainfall mapping using multiple evaluation criteria and auxiliary data sources: A case study of Sri Lanka. *Environmental Modelling & Software*, *67*, pp.57-71. doi.org/10.1016/j.envsoft.2015.01.011.

31- Rousta, I., Doostkamian, M., Haghighi, E., Ghafarian Malamiri, H.R. and Yarahmadi, P., 2017. Analysis of spatial autocorrelation patterns of heavy and super-heavy rainfall in Iran. A*dvances in Atmospheric Sciences*, 34, pp.1069-1081.

32- Saatsaz, M., 2020. A historical investigation on water resources management in Iran. *Environment, Development and Sustainability*, *22*(3), pp.1749-1785.

33- Schaback, R., 2005. Multivariate interpolation by polynomials and radial basis functions. *Constructive Approximation*, *21*(3), pp.293-317.

34- Shepard, D., 1968, January. A two-dimensional interpolation function for irregularly-spaced data. In *Proceedings of the 1968 23rd ACM national conference* (pp. 517-524). doi.org/10.1145/800186.810616.

35- Swan, A., 1998. GOOVAERTS, P. 1997. Geostatistics for Natural Resources Evaluation. Applied Geostatistics Series. xiv+ 483 pp. New York, Oxford: Oxford University Press. Price£ 46.95 (hard covers). ISBN 0 19 511538 4. *Geological Magazine*, *135*(6), pp.819-842.

36- Vicente-Serrano, S.M., Saz-Sánchez, M.A. and Cuadrat, J.M., 2003. Comparative analysis of interpolation methods in the middle Ebro Valley (Spain): application to annual precipitation and temperature. *Climate research*, *24*(2), pp.161-180.

37- WILLMOTT, C. J. 1982. Some comments on the evaluation of model performance. *Bulletin of the American Meteorological Society,* 63, 1309-1313. doi:10.3354/cr024161.

38- Xu, W., Zou, Y., Zhang, G. and Linderman, M., 2015. A comparison among spatial interpolation techniques for daily rainfall data in Sichuan Province, China. *International Journal of Climatology*, *35*(10), 2898-2907. doi.org/10.1002/joc.4180.

39- Yang, X., Xie, X., Liu, D.L., Ji, F. and Wang, L., 2015. Spatial interpolation of daily rainfall data for local climate impact assessment over greater Sydney region. *Advances in Meteorology*, *2015*(1), p.563629. doi.org/10.1155/2015/563629.

40- Zimmerman, D., Pavlik, C., Ruggles, A. and Armstrong, M.P., 1999. An experimental comparison of ordinary and universal kriging and inverse distance weighting. *Mathematical Geology*, *31*, pp.375-390.